Plasmonics (2013) 8:749–754
DOI 10.1007/s11468-012-9467-9

Ferroelectric Hybrid Plasmonic Waveguide for All-Optical Logic Gate Applications

Cuicui Lu · Xiaoyong Hu · Song Yue · Yulan Fu · Hong Yang · Qihuang Gong

Received: 2 September 2012 / Accepted: 19 November 2012 / Published online: 28 November 2012

Abstract A ferroelectric hybrid plasmonic waveguide, made of a polycrystal lithium niobate waveguide separated from a gold film by a silicon dioxide isolation layer, is fabricated by use of laser molecular beam epitaxy growth, electron beam evaporation, and focused ion beam etching. Strong subwavelength mode confinement and excellent long-range propagation are achieved simultaneously for the hybrid plasmonic mode. An all-optical logic OR gate is also realized based on the ferroelectric hybrid plasmonic waveguide. This may provide a way for the study of all-optical logic gates and integrated photonic circuits.

Keywords Hybrid plasmonic waveguide · All-optical logic gate · Surface plasmon polariton

PACS numbers 42.79.Ta · 78.67.Pt · 81.07.-b

Introduction

Nanoscale optical waveguide is a basic element for optical interconnection networks and integrated photonic circuits. There are mainly three kinds of nanoscale waveguides: silicon-on-insulator nanowires with an ultrahigh refractive index contrast [1], photonic crystal waveguide [2], and surface plasmon (SP) waveguides [3]. For the former two nanoscale waveguides, the optical filed is limited to the order of the wavelength. The SP waveguide can provide a subwavelength confinement; however, the propagation distance is just several micrometers due to the strong optical losses of metal. In 2008, Oulton et al. proposed a hybrid plasmonic waveguide for subwavelength confinement and long-range propagation, i.e., when depositing a low and high refractive index dielectric layers on a metal film, the electric field of plasmonic modes will be pulled from the metal surface and confined in the low index dielectric layer [4]. The hybrid plasmonic waveguide has attracted great interest due to its excellent subwavelength confinement and long-range propagation properties [5–7]. However, to date, only limited experimental results were reported because the fabrication of the hybrid plasmonic waveguide is very difficult. In 2010, Kim et al. reported a polymer hybrid plasmonic waveguide constructed by embedding a gold stripe in a dual dielectric slab waveguide made of UV-curable polymer FOWG [8]. Recently, Lou et al. realized a compact directional couplers based on a silicon hybrid plasmonic waveguide [9]. Up to now, little attention was paid to the applications of hybrid plasmonic waveguides in nanoscale-integrated all-optical logic devices, which are essential components of optical computing systems.

Here, we study how to realize nanoscale all-optical logic gate devices based on a ferroelectric hybrid plasmonic waveguide, which consists of a polycrystalline lithium niobate ($LiNbO_3$) waveguide separated from a gold film by a silicon dioxide (SiO_2) layer. Strong subwavelength mode confinement and excellent long-range propagation properties are achieved simultaneously for hybrid plasmonic modes. For the hybrid plasmonic mode with a wavelength of 575 nm, the effective mode area and the propagation length reach $\lambda^2/82$ and 23 μm, respectively. Moreover, nanoscale crystal grains of polycrystalline $LiNbO_3$ can provide excellent third-order optical nonlinearity because of the quantum confinement effect [10, 11], which also offer an approach to reaching ultrafast all-optical tunable photonic devices. An all-optical logic OR gate was realized based on the ferroelectric hybrid plasmonic waveguide.

C. Lu · X. Hu (✉) · S. Yue · Y. Fu · H. Yang · Q. Gong (✉)
State Key Laboratory for Mesoscopic Physics & Department of Physics, Peking University, Beijing 100871, Peoples Republic of China
e-mail: xiaoyonghu@pku.edu.cn
e-mail: qhgong@pku.edu.cn

Structure Design

The schematic structure of the ferroelectric hybrid plasmonic waveguide is shown in Fig. 1a. The ferroelectric hybrid plasmonic waveguide was composed of a SiO_2 layer sandwiched between a polycrystalline $LiNbO_3$ waveguide and gold film on the silicon dioxide substrate. The thickness was 360 nm for gold film, 125 nm for SiO_2 layer, and 110 nm for the polycrystalline $LiNbO_3$ layer. The width of the polycrystalline $LiNbO_3$ waveguide was 350 nm. The finite element method (using a commercial software COMSOL Multiphysics) was adopted to study the light confinement and propagation properties of the ferroelectric hybrid plasmonic waveguide. The refractive index of polycrystalline $LiNbO_3$ and SiO_2 was measured to be 2.297 and 1.441, respectively, by using an ellipsometer. The wavelength-dependent complex refractive index of gold was obtained from the Ref. [12]. Owing to the strong coupling of surface plasmon polariton (SPP) modes provided by the gold film and waveguide modes provided by the polycrystalline $LiNbO_3$ layer, two degenerate hybrid plasmonic modes with a resonant wavelength of 575 nm, i.e., an even mode with its polarization in the vertical direction and an odd mode with its polarization in the horizontal direction, can be obtained in the ferroelectric hybrid plasmonic waveguide [4]. In our experiment, we only excited the even hybrid plasmonic mode. The calculated field distribution of Ey component of the even mode by the finite element method is shown in Fig. 1b. It is clear that the electric field distribution is confined to the low refractive index SiO_2 layer. The reason lies in the requirement of the continuity of the displacement field at the material interfaces, which results in a strong normal electric field component in the low refractive index isolation region [4]. The effective mode size was calculated to be 375 nm along the X direction and 125 nm along the Y direction, respectively. This corresponds to an effective mode area of $\lambda^2/82$, which indicates a strong subwavelength mode confinement [13]. To confirm the light confinement properties, we calculated the magnitude of Ey component of the hybrid plasmonic even mode by the finite element method, and the calculated result is shown in Fig. 1c. The proportion of the mode's energy residing within the SiO_2 layer reached 71 %, which confirms the strong mode confinement of ferroelectric plasmonic waveguide. To study the propagation properties of the ferroelectric hybrid plasmonic waveguide, we calculated the changes of the power flow of the hybrid plasmonic even mode with propagation distance by the finite element method, and the calculated results are shown in Fig. 1d. The propagation length L of the hybrid plasmonic mode, defined as the distance when the power flow attenuates to $1/e$ of the maximum value, can be obtained from the exponentially fitted result. The propagation length was 23.3 μm. The effective refractive index n_{eff} was $1.443–0.002728i$ for the 575-nm hybrid plasmonic mode. These evidences indicate that the ferroelectric hybrid plasmonic waveguide can provide strong subwavelength mode confinement and long-range propagation for the 575-nm hybrid plasmonic mode.

Experimental Method

A laser molecular beam epitaxy (LMBE) growth system (model LMBE 450, SKY Company, China) was used to

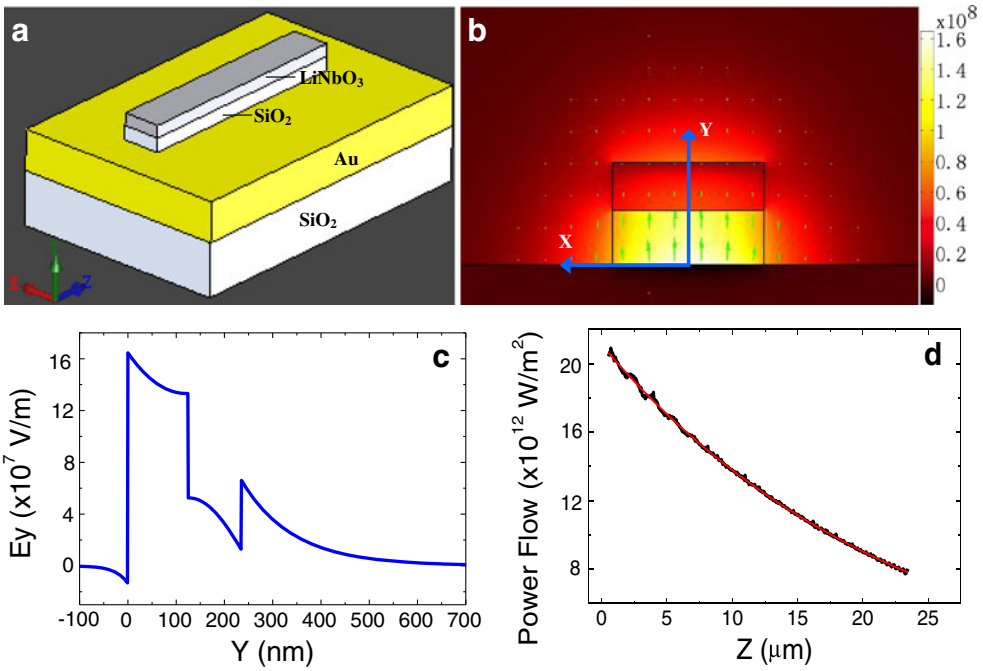

Fig. 1 **a** Schematic structure of the ferroelectric hybrid plasmonic waveguide. **b** Field distribution of the Ey component. The *green arrows* are the polarization directions. **c** The magnitude of Ey along Y direction when X=0. **d** Calculated power flow changes with the propagation distance. The *red line* is the exponentially fitted result

fabricate the 360-nm thick gold film on silicon dioxide substrates and the 110-nm thick polycrystalline $LiNbO_3$ layer. The beam (with a wavelength of 248 nm, a pulse energy of 500 mJ, and a pulse repetition rate of 5 Hz) output from an excimer laser system (model COMPexPro 205, Coherent Company, USA) was used as the excitation light source. The beam was focused onto a gold target (or a $LiNbO_3$ ceramic target) mounted on a rotating holder, 7.95 cm away from the silica substrate. The 125-nm thick SiO_2 isolation layer was fabricated by using an electron beam evaporation system (Edwards BOC 500, UK). The quality of the fabricated films was characterized by using an atomic force microscope system (model MFP-3D, Asylum Company, USA). The atomic force microscopy (AFM) image of the 360-nm thick gold film is shown in Fig. 2a. The average surface roughness was less than 3 nm. The AFM image of the 125-nm thick SiO_2 isolation layer is shown in Fig. 2b. The average surface roughness was less than 5 nm. The AFM image of the 110-nm thick $LiNbO_3$ layer is shown in Fig. 2c. The $LiNbO_3$ film took on the configuration of a polycrystal, constructed from small crystal grains with an average diameter of about 100 nm, which can provide strong quantum confinement-enhancing nonlinearity effect [10, 11]. The average surface roughness was less than 10 nm. A focused ion beam (FIB) etching system (model DB235, FEI Company, USA) was used to prepare the patterns of the hybrid plasmonic waveguide.

Results and Discussions

The scanning electron microscopy (SEM) image of the fabricated ferroelectric hybrid plasmonic straight waveguide sample is shown in Fig. 3a. The whole hybrid plasmonic waveguide structure was composed of the coupling grating port (Fig. 3c), the straight waveguide, and the decoupling grating port (Fig. 3d). As for the preparation of the straight waveguide, both the dielectric layers (including $LiNbO_3$ and SiO_2 layers) on the up- and downside are removed through the FIB etching, and only a center dielectric $LiNbO_3$–SiO_2 stripe waveguide has remained on the gold film. The width and length of the ferroelectric hybrid plasmonic straight waveguide were 350 nm and 20 μm, respectively. As for the preparation of the coupling grating port, both the dielectric layers (including $LiNbO_3$ and SiO_2 layers) in a rectangular area (6×4 μm) were removed, and subsequently, three one third circular air grooves were etched through the gold film. The grating period and the air groove width were 830 and 160 nm, respectively. The circular grooves have the same circle center at the start point of the straight waveguide, as shown in Fig. 3c. It has been pointed out that the plasmonic lens consisting of ring grooves perforated in metallic film can efficiently couple free space propagating

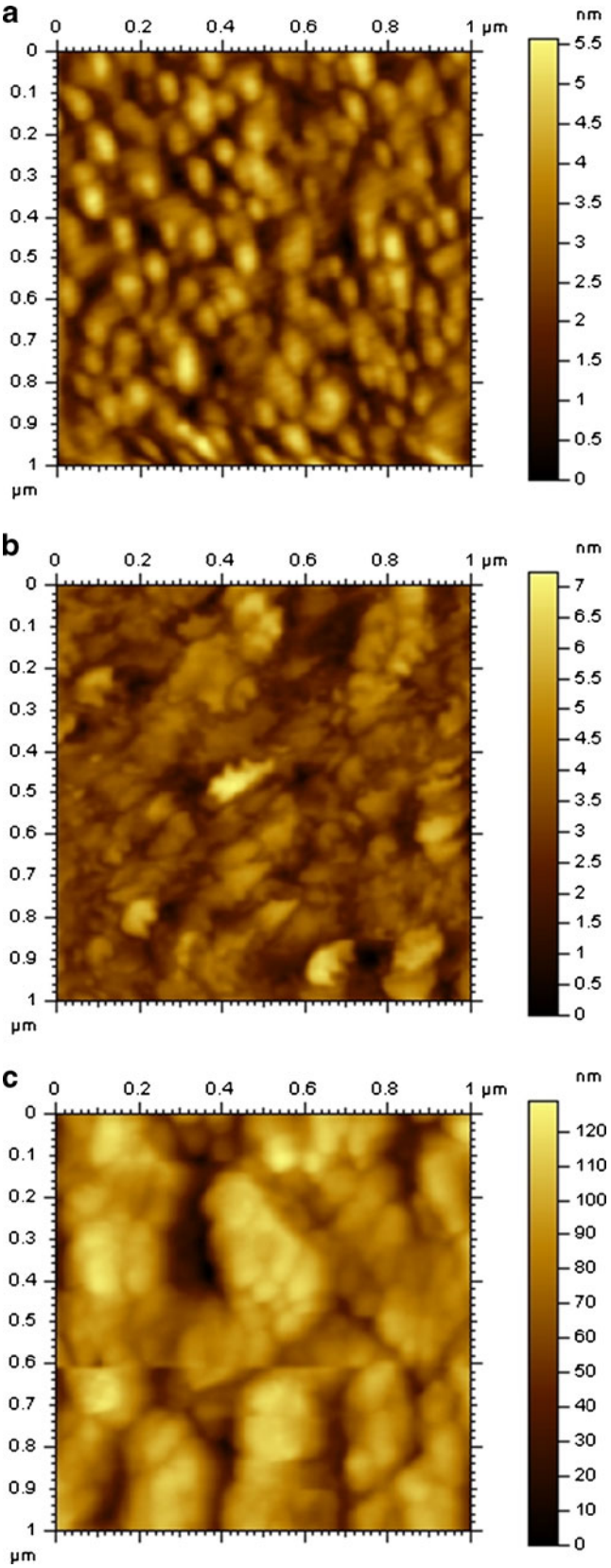

Fig. 2 AFM images for a 360-nm thick gold film (**a**), a 125-nm thick SiO_2 film (**b**), and a polycrystal $LiNbO_3$ film (**c**)

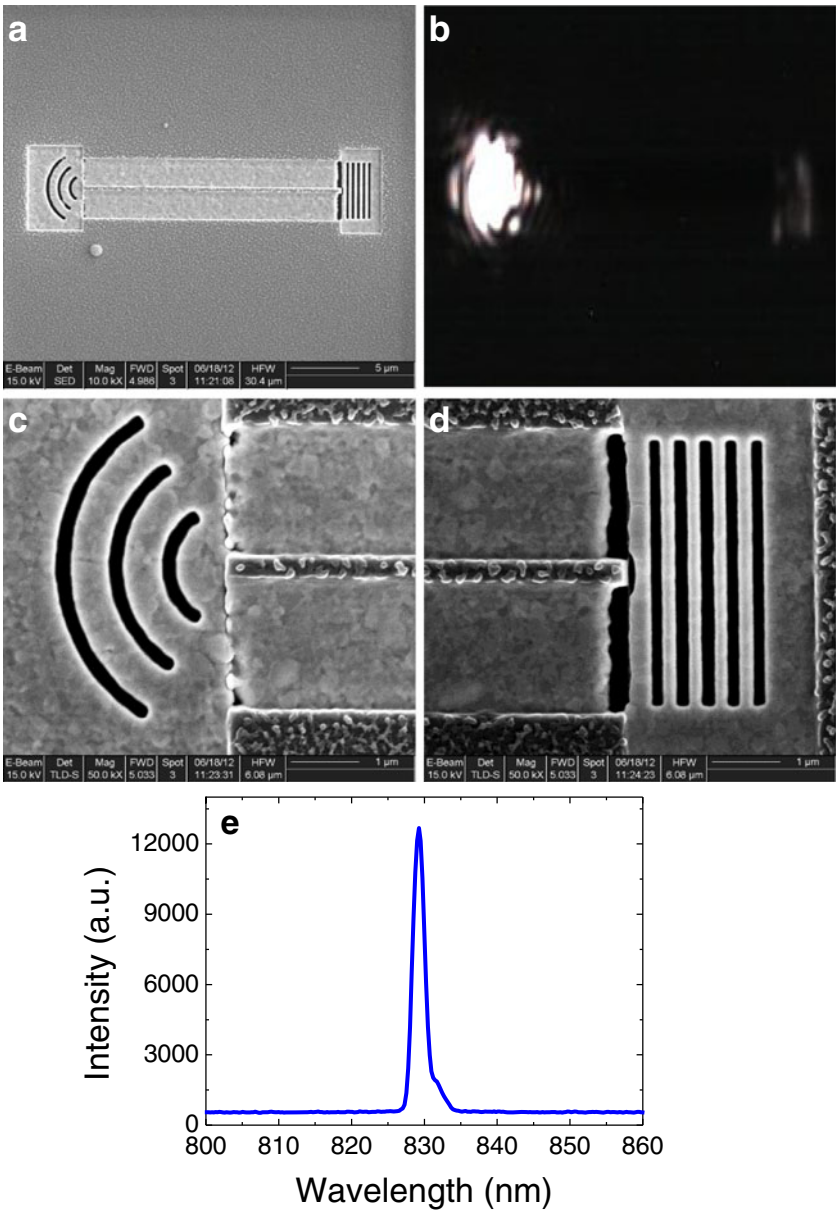

Fig. 3 **a** SEM images of the ferroelectric hybrid plasmonic straight waveguide. **b** CCD image of ferroelectric hybrid plasmonic waveguide under excitation of an 830-nm CW laser. **c** SEM image of the coupling grating port. **d** SEM image of the decoupling grating port. **e** Spectrum of the 830-nm CW laser

light into a subdiffraction-limited focusing spot of SPP modes [14–16]. Compared with the prism-coupling method and the end-fire coupling method, the method used in our experiment is more efficient and easy to perform [17–19]. The fabrication process of the decoupling grating port was similar to that of the coupling grating port. The decoupling grating port consists of five straight air grooves to help couple the energy of the hybrid plasmonic mode to the free space for the purpose of measurement.

The propagation properties of the ferroelectric hybrid plasmonic waveguide were measured by the use of a scanning near-field optical microscopy system. The input coupling grating was normally illuminated from the back side using a horizontally polarized continuous wave (CW) laser beam (Ti: sapphire laser, model Mira 900F, Coherent Company, USA) with a wavelength of 830 nm. The beam radius was focused to about 3 μm by a ×100 microscope objective. The SPP mode was generated in the interface between gold and air in the grooves, thus the polarization of the electric field was in the vertical direction when the SPP mode was focused on the start point of the waveguide (the circle center), which has been confirmed by Li's calculations [16]. The spectrum of the 830-nm laser beam is shown in Fig. 3e. The linewidth of the laser spectrum curve was only 1.9 nm, which ensured that only the needed quasi-monochromatic 575-nm hybrid plasmonic mode can be excited in the ferroelectric hybrid plasmonic waveguide. The hybrid plasmonic mode propagating through the ferroelectric hybrid plasmonic waveguide was scattered by the decoupling grating in the output port. The scattered light was collected by a long working distance objective (Mitutoyo

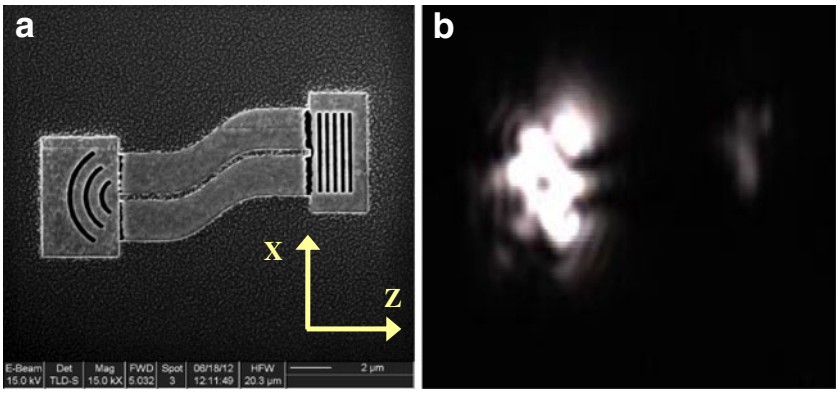

Fig. 4 SEM images for the ferroelectric hybrid plasmonic bend waveguide (**a**) and CCD image of the ferroelectric hybrid plasmonic bend waveguide under excitation of an 830-nm CW laser (**b**)

20, NA=0.58) and then imaged onto a charge-coupled device (CCD) camera. The measured CCD image of the ferroelectric hybrid plasmonic straight waveguide is shown in Fig. 3b. It is very clear that under excitation of an 830-nm CW laser, there is obvious signal output from the decoupling grating. The 575-nm hybrid plasmonic mode can propagate at least 20 μm, which provides a perfect platform for the realization of ultracompact all-optical logic devices. To further confirm the propagation properties of the hybrid plasmonic mode in the ferroelectric hybrid plasmonic waveguide, we also etched a sinusoidal bend waveguide, as shown in Fig. 4a. The total length of the bend waveguide is 10 μm in the *Z* direction, having a sinusoidal turning with a length of 6 μm in the *Z* direction and 2.25 μm in the *X* direction. The measured CCD image of the ferroelectric hybrid plasmonic bend waveguide is shown in Fig. 4b. Under excitation of an 830-nm CW laser, there is obvious signal output from the decoupling grating. This confirms the excellent propagation properties of the 575-nm hybrid plasmonic mode in the ferroelectric hybrid plasmonic waveguide. The input and output signal intensities of the ferroelectric hybrid plasmonic waveguide can be extracted from the CCD image obtained under excitation of an 830-nm CW laser [20]. From the CCD image shown in Fig. 3b, the measured input and output signal intensities of the ferroelectric hybrid plasmonic waveguide were 402,526 and 41,989 a.u., respectively. The output signal intensity does not agree well with the theoretical result, i.e., 1/e times of the input signal intensity. The reason may lie in the following factors: Firstly, the configuration of the coupling grating in the input port was different from that of the decoupling grating in the output port.

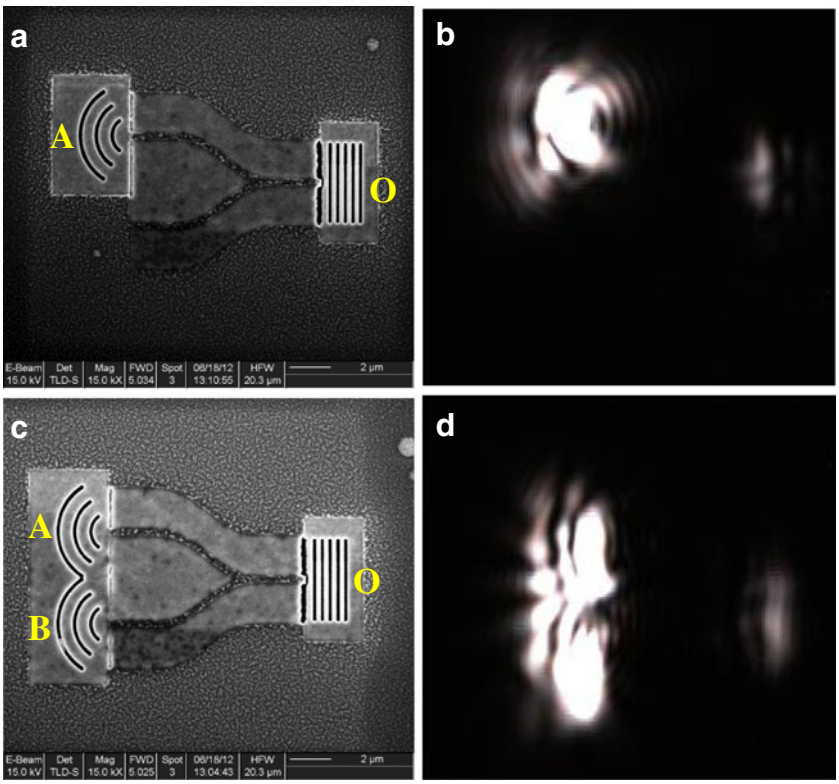

Fig. 5 Logic operation of all-optical logic OR gate. The SEM image of sample (**a**), measured CCD image under excitation of an 830-nm CW laser (**b**) for the logic operation of 1 OR 0=1. The SEM image of sample (**c**), measured CCD image under excitation of an 830-nm CW laser (d) for the logic operation of 1 OR 1=1. The indicators "A, B and O" help to understand the logic operation

This makes that the generation efficiency is different from the decoupling efficiency for the hybrid plasmonic modes. Secondly, the upper $LiNbO_3$ layer takes on the configuration of polycrystalline, which increases the propagation losses of hybrid plasmonic modes.

An all-optical logic OR gate was fabricated by the use of FIB etching based on the ferroelectric hybrid plasmonic waveguide. The OR gate has a symmetric "Y" shape configuration, as shown in Fig. 5a, c; the bending region of which having a sinusoidal shape so as to reduce the propagation losses [21]. The distance between waveguide A and B was near 3 μm. The length of the bended waveguide was 10 μm. The distance from the input port of waveguide A and B to the interaction point has exactly the same value, which ensures a constructive interference in the output waveguide. To perform the logic operation of "1 OR 0 =1," we etched a coupling grating in the input port of the waveguide A, as shown in Fig. 5a. The 575-nm hybrid plasmonic mode can only be excited in the waveguide A. The measured CCD image under excitation of an 830-nm CW laser is shown in Fig. 5b. There is a strong signal output from the decoupling grating, which corresponds to the output logic 1. To perform the logic operation of "1 OR 1=1," we etched a coupling grating in the input port of both waveguide A and B, as shown in Fig. 5c. The 575-nm hybrid plasmonic mode can be excited in waveguide A and B simultaneously. The measured CCD image under excitation of an 830-nm CW laser is shown in Fig. 5d. There is a very strong signal output from the decoupling grating, which corresponds to the output logic 1. The reason is that a constructive interference is reached in the output waveguide for the hybrid plasmonic modes propagating through waveguides A and B due to the zero optical path difference.

Conclusions

In conclusion, a ferroelectric hybrid plasmonic waveguide with strong subwavelength confinement and long-range propagation was realized. The effective mode area and the propagation length reached $\lambda^2/82$ and 23 μm, respectively. An all-optical logic OR gate is also realized. This may be a useful reference for the study of nanoscale-integrated all-optical logic device and integrated photonic circuits.

Acknowledgments This work was supported by the National Basic Research Program of China under grant 2013CB328704, the National Natural Science Foundation of China under grants 61077027, 11134001, 11121091, and 90921008, and the program for New Century Excellent Talents in University.

References

1. Almeida VR, Xu Q, Barrios CA, Lipson M (2004) Guiding and confining light in void nanostructure. Opt Lett 29:1209–1211
2. Mekis A, Chen JC, Kurland I, Fan SH, Villeneuve PR, Joannopoulos JD (1996) High transmission through sharp bends in photonic crystal waveguides. Phys Rev Lett 77:3787–3790
3. Bozhevolnyi SI, Volkov VS, Devaux E, Laluet JY, Ebbesen TW (2006) Channel plasmon subwavelength waveguide components including interferometers and ring resonators. Nature 440:508–511
4. Oulton RF, Sorger VJ, Genov DA, Pile DFP, Zhang X (2008) A hybrid plasmonic waveguide for subwavelength confinement and long-range propagation. Nat Photon 2:496–500
5. Dai DX, He SL (2009) Asilicon-based hybrid plasmonic waveguide with a metal cap for a nano-scale light confinement. Opt Express 17:16646–16653
6. Alam MZ, Meier J, Aitchison JS, Mojahedi M (2010) Propagation characteristics of hybrid modes supported by metal-low-high index waveguides and bends. Opt Express 18:12971–12979
7. Dai DX, He SL (2010) Low-loss hybrid plasmonic waveguide with double low-index nano-slots. Opt Express 18:17958–17966
8. Kim JT, Ju JJ, Park S, Kim MS, Park SK, Shin SY (2010) Hybrid plasmonic waveguide for low-loss lightwave guiding. Opt Express 18:2808–2813
9. Lou F, Wang ZC, Dai DX, Thylen L, Wosinski L (2012) Experimental demonstration of ultra-compact directional couplers based on silicon hybrid plasmonic waveguides. Appl Phys Lett 100:241105
10. Wang QQ, Wang SF, Huang WT, Gong QH, Yang BF, Shi J (2002) Ultrafast and large third-order optical nonlinearity of porous nano-sized polycrystal $LiNbO_3$ film. J Phys D: Appl Phys 35:430–432
11. Hu XY, Zhang YB, Fu YL, Yang H, Gong QH (2011) Low-power and ultrafast all-optical tunable nanometer-scale photonic metamaterials. Adv Mater 23:4295–4300
12. Weber MJ (2003) Handbook of optical materials. CRC Press, Berkley
13. Chen JJ, Li Z, Yue S, Gong QH (2009) Hybrid long-range surface plasmon-polariton modes with tight field confinement guided by asymmetrical waveguides. Opt Express 17:23603–23609
14. Nomura W, Ohtsu M (2005) Nanodot coupler with a surface plasmon polariton condenser for optical far/near-field conversion. Appl Phys Lett 86:181108
15. Yue S, Li Z, Chen JJ, Gong QH (2011) Ultrasmall and ultrafast all-optical modulation based on a plasmonic lens. Appl Phys Lett 98:161108
16. Li XW, Huang LL, Tan QF, Bai BF, Jin GF (2011) Integrated plasmonic semi-circular launcher for dielectric-loaded surface plasmon-polariton waveguide. Opt Express 19:6541–6548
17. Holmgaard T, Bozhevolnyi SI, Markey L, Dereux A, Krasavin A, Bolger P, Zayats A (2008) Efficient excitation of dielectric-loaded surface plasmon-polariton waveguide modes at telecommunication wavelengths. Phys Rev B 78:165431
18. Gosciniak J, Volkov VS, Bozhevolnyi SI, Markey L, Massenot S, Dereux A (2010) Fiber-coupled dielectric-loaded plasmonic waveguides. Opt Express 18:5314–5319
19. Grandidier J, Francs GCD, Massenot S, Bouhelier A, Markey L, Weeber JC, Finot C, Dereux A (2009) Gain-assisted propagation in a plasmonic waveguide at telecom wavelength. Nano Lett 9:2935–2939
20. Chen JJ, Li Z, Yue S, Gong QH (2011) Highly efficient all-optical control of surface-plasmon-polariton generation based on a compact asymmetric single slit. Nano Lett 11:2933–2937
21. Volkov VS, Bozhevolnyi SI, Devaux E, Ebbesen TW (2006) Compact gradual bends for channel plasmon polaritons. Opt Express 14:4494–4503